Understanding the Geophysical Sources of Uncertainty for Satellite Interferometric (SRTM)-Based Discharge Estimation in River Deltas: The Case for Bangladesh

Md. Safat Sikder and Faisal Hossain

***Abstract*—Like most river deltas, Bangladesh represents a geographically small region with numerous crisscrossing rivers. The total number of rivers in Bangladesh exceeds 300, of which 57 rivers are transboundary. Given the widespread unavailability of flow data across the entire river basins of Ganges, Brahmaputra, and Meghna, combined with a declining measurement network and political challenges of sharing the data, satellite remote sensing of discharge has recently become a viable alternative. This study was motivated by the need to understand the geophysical sources of uncertainty of satellite interferometric-based discharge estimation in Bangladesh. A consequential goal of this study was to contextualize the understanding as a function of river's geophysical characteristics (river width, reach averaging length, and bed/water slope) and also to explore a pragmatic approach to uncertainty reduction using water level climatology. Discharge was estimated according to the slope-area (Manning's) method using elevation data from Shuttle Radar Topography Mission (SRTM). A high-resolution hydrodynamic (HD) model was accurately calibrated to simulate water level and flow dynamics along the river reaches of the river network and serve as reference for comparison with satellite-based estimates. It was found that satellite interferometric (SRTM)-based discharge estimates yielded estimation error variance an order smaller than the natural flow variability only if the river width was at least three times larger the width of the native resolution of satellite elevation data. Rivers narrower than this width (for SRTM, this cutoff is 270 m) yielded a coefficient of variation larger than 1 due to contamination of land elevation data in hydraulic parameter calculations. It was also found that water level climatology can be useful in significantly reducing the estimation uncertainty for these narrow rivers. While reach averaging length appeared insensitive to accuracy for wide rivers (width >1 km), a few rivers seemed to have an optimal reach averaging length at which the highest accuracy is obtained. Finally, it was found that if reach-averaged hydraulic parameters (area, slope, and radius) are used for the calculation of reach-averaged discharge, the needed linear (bias) correction factors, although unique and arbitrary for each river reach, can improve accuracy of flow simulations.**

***Index Terms*—Discharge estimation, hydrodynamic (HD) model, interferometry, Manning's approach, uncertainty.**

Manuscript received February 03, 2014; revised May 06, 2014; accepted May 15, 2014. This work was support in part by the NASA Physical Oceanography program (NN13AD97G) and in part by the NASA SERVIR program (NNX12AM85AG). The work of M. S. Sikdar was supported in part by the Ivanhoe Foundation.

The authors are with the Civil and Environmental Engineering Department, University of Washington, Seattle, WA 98195 USA (e-mail: safatbd@gmail.com; fhossain@uw.edu).

Color versions of one or more of the figures in this paper are available online at http://ieeexplore.ieee.org.

Digital Object Identifier 10.1109/JSTARS.2014.2326893

I. Introduction

BANGLADESH is a low-lying delta in the foothills of the Himalayan Mountains. Like most river deltas, it represents a geographically small region with numerous crisscrossing rivers. The total number of rivers in Bangladesh exceeds 300 (Fig. 1). Among them, 57 rivers are transboundary—i.e., they cross the international border with Bangladesh. Of these, only three flow from Myanmar, whereas the rest drain into Bangladesh from India. The three major rivers, Ganges, Brahmaputra, and Meghna rivers, drain about $1.72\ \text{million km}^2$ of catchment area and yet only 7% of the area is within the country (http://www.jrcb.gov.bd/) [12].

The average annual flow through the Ganges river is about $12\,120\ \text{m}^3/\text{s}$, Brahmaputra river is about $19\,200\ \text{m}^3/\text{s}$, and the Meghna river is about $3510\ \text{m}^3/\text{s}$ [23]. However, this average flow belies the one order of inter-annual variability that these rivers experience. For example, the total flow of these three major rivers during February is $18\,200\ \text{m}^3/\text{s}$, which then gradually rises to $243\,500\ \text{m}^3/\text{s}$ during August [24].

Almost every year Bangladesh suffers from flooding. The low-frequency floods of recent years have occurred in 1954, 1955, 1970, 1974, 1984, 1987, 1988, 1998, 2004, and 2007 [8], [16]. Such flooding mainly takes place when the peak discharges in the Brahmaputra, the Ganges, and the Meghna rivers coincide at the confluence (the Meghna Estuary) before draining into the Bay of Bengal. Twenty percent of the country is usually inundated with the average annual flood, whereas the less frequent but more extreme floods typically inundate more than 35% of the area [16].

Bangladesh adopts both structural and nonstructural measures to mitigate flood damage. Among the nonstructural measures, the Flood Forecasting and Warning Center (FFWC; www.ffwc.gov.bd) is mandated with producing flood forecasts using a combination of hydrologic model and country-wide *in situ* rainfall/flow measurement network [6]. However, due to unavailability of data on discharge from the upstream transboundary region of Bangladesh (which represents 90% of the total drainage area), FFWC is only able to forecast up to 3-day lead time [25].

Under such a scenario of data unavailability, remote sensing can be an alternative source. For example, the Scanning Multichannel Microwave Radiometer (SMMR) on Nimbus-7 is an example of a passive microwave (PMW) sensor that can be used to determine the seasonal inundation pattern of rivers [32]. The radar altimeters on board Topex/POSEIDON [3], ERS1/2 [4], [30], ENVISAT [30], and JASON [27] are also proficient in

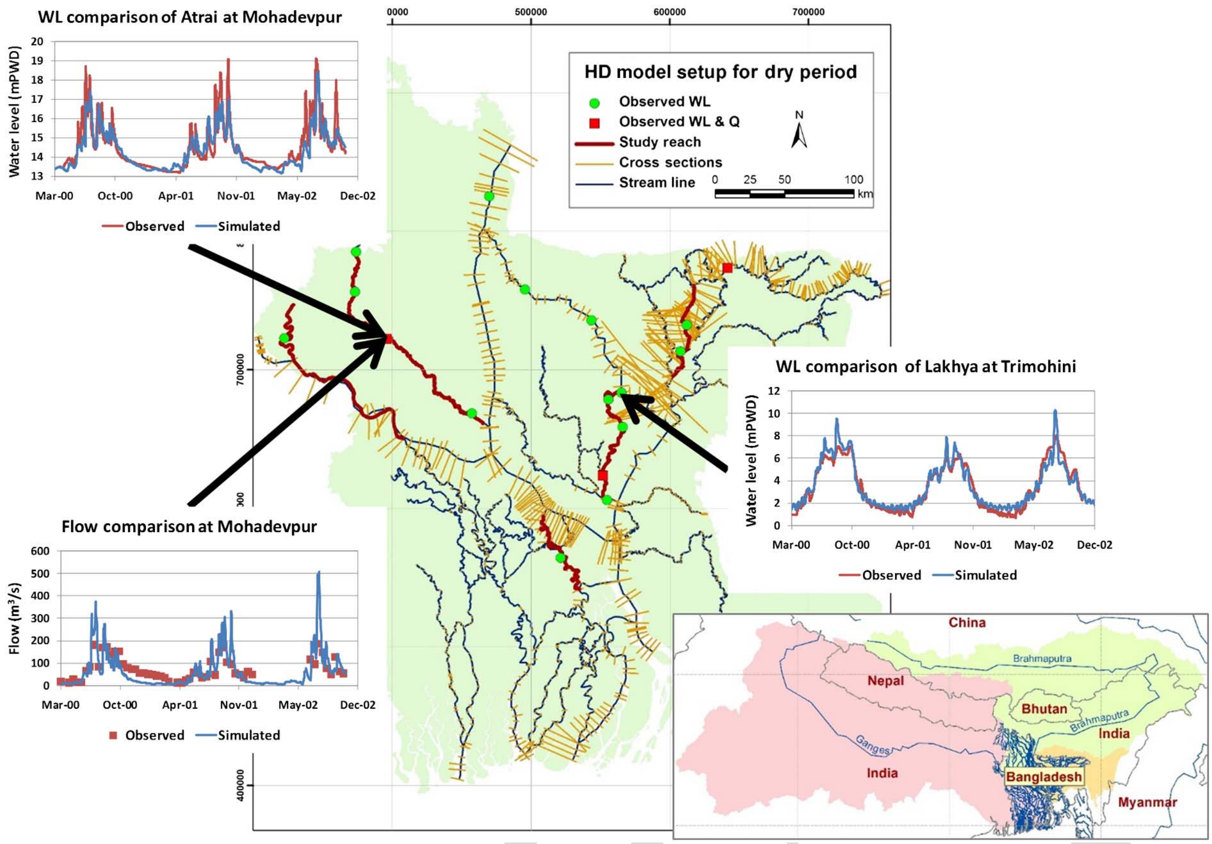

Fig. 1. Calibration of the HEC-RAS (HD) showing the level of match at two key river locations for two unique rivers during the period of 2000–2002. The highlighted reaches shown in thick red lines represent the study reaches. Note: The flow observations for Mohadevpur are not continuous and are often biweekly.

measuring water level of wide rivers [29]. Synthetic aperture radars (SARs) such as ERS-1 [11], JERS-1 [33], and RADARSAT [35] are capable of measuring inundation during any weather condition [22], [32].

Discharge, however, cannot be directly measured by any remote sensing technique. As discharge represents the flux of water though a channel cross-sectional area, a combination of spaceborne observables such as water level (h), river width (w), surface water slope (∂h/∂x), sinuosity, and water body area need to be used to estimate discharge [22]. A thorough review of various approaches to determine discharge from space is provided in [1], which has recently been revisited and updated in [28]. For example, discharge can be estimated from the fluvial surface velocity of rivers using airborne data (e.g., [7]) or spaceborne data [26]. Discharge can also be determined by regression analysis of spaceborne measurement of river width or inundated area with *in situ* discharge data (e.g., [31]) or with estimated shoreline elevation (e.g., [5]). Another approach is regression analysis of radar altimeter and *in situ* measured discharge (e.g., [17]). Among currently used techniques, one of the more physically grounded approaches is that using Manning's equation to derive discharge from spaceborne-derived water surface slope and stage data using satellite interferometry (e.g., [9], [15], [19], and [34]).

The water surface slope-based discharge estimation technique using the Manning's equation has particular importance due to the upcoming Surface Water Ocean Topography (SWOT) mission. The SWOT mission will use a new type of Ka band radar interferometer (KaRIN), which will be mounted on either side of a 10 m long mast and will cover a 120 km wide swath [1] (http://swot.jpl.nasa.gov). With significantly higher quality water surface elevation image data on rivers and water bodies that is anticipated from the SWOT mission on a global and routine scale, it should be possible to improve the skill of the forecasting system for transboundary floods for Bangladesh [2], [13].

The basic inputs in Manning's equation to calculate discharge from satellite interferometry of elevation are: water surface slope (S_o) instead of friction slope (S_f), cross-sectional area (A), Manning's n as roughness of the channel and hydraulic radius (R), which can be derived from wetted perimeter (P), and cross-sectional area (A). Stage (h) and slope (S_o) can be derived from radar interferometry and cross-sectional area (A), wetted perimeter (P) can be determined using stage (h), if *in situ* bathymetry is available. Manning's n can be assumed (or calibrated) to derive discharge. For scenarios where *in situ* bathymetry is unavailable, Durand *et al.* [9], among others, have proposed a technique for discharge estimation by invoking the continuity equation or alternative approaches.

However, due to the inherent uncertainty in measurement of spaceborne water elevation and river width parameters, errors propagate to estimated discharge regardless of the technique used. In addition, reach averaging is also required for slope ($\partial h/\partial x$) calculation, which consequently is likely to have a direct impact on the derived slope. Thus, accuracy of spaceborne

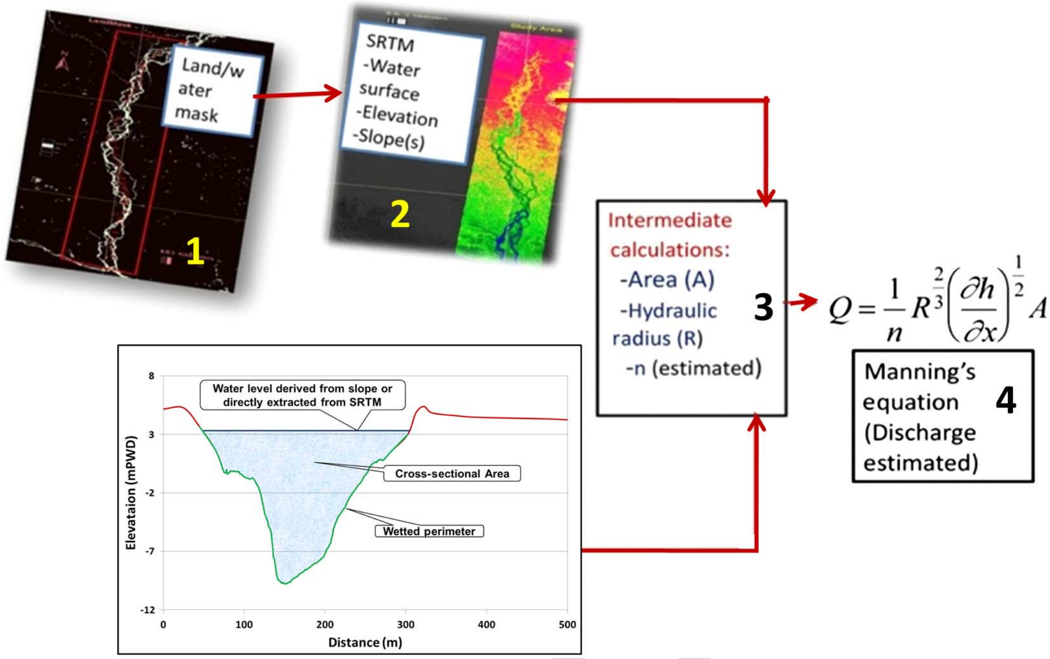

Fig. 2. Steps to satellite-based discharge estimation using SRTM elevation data, *in situ* bathymetry, and Manning's equation (after Woldemichael *et al.* [34]).

estimated discharge can depend on various factors ranging from the derived slope, reach averaging length, derived water elevation, and river width. In [34], Woldemichael *et al.* showed a sensitivity analysis of change of section factor ($AR^{2/3}$) along the river reach. They suggest that the use of minimum water level for low-flow regimes can alleviate the uncertainty that can arise from uncertainty in section factor estimation. In general, a broader understanding is required for these controlling factors, namely the geophysical sources that dictate the accuracy of satellite discharge estimation using the slope-area method of Manning's equation. This understanding is critical to set the stage for improvement of algorithms during the SWOT era building on existing approaches that do not depend on the need for *in situ* bathymetry measurements (such as [9] and [20]).

This study is motivated by the need to understand the river's geophysical sources of uncertainty for satellite interferometric-based discharge estimation in the river delta of Bangladesh. A consequential goal of this study is to contextualize the understanding as a function of river characteristics (river width, flow regime, and bed slope) and also to explore a pragmatic approach of uncertainty reduction using flow climatology. Until SWOT becomes a reality, the only global source of satellite interferometric elevation data of water bodies that is also the closest analog to the SWOT mission is the SRTM, albeit with significant difference in scale, precision, and accuracy. Jung *et al.* [15] and Woldemichael *et al.* [34] recently reported a case study on the Brahmaputra river using the SRTM measurements of $\partial h/\partial x$. This one-time SRTM mission (which flew over Bangladesh on February 20, 2000) provided a global coverage of digital elevation data using interferometry. Nevertheless, this study is expected to have value for SWOT if we are mindful of the following caveats (i.e., premise) that apply.

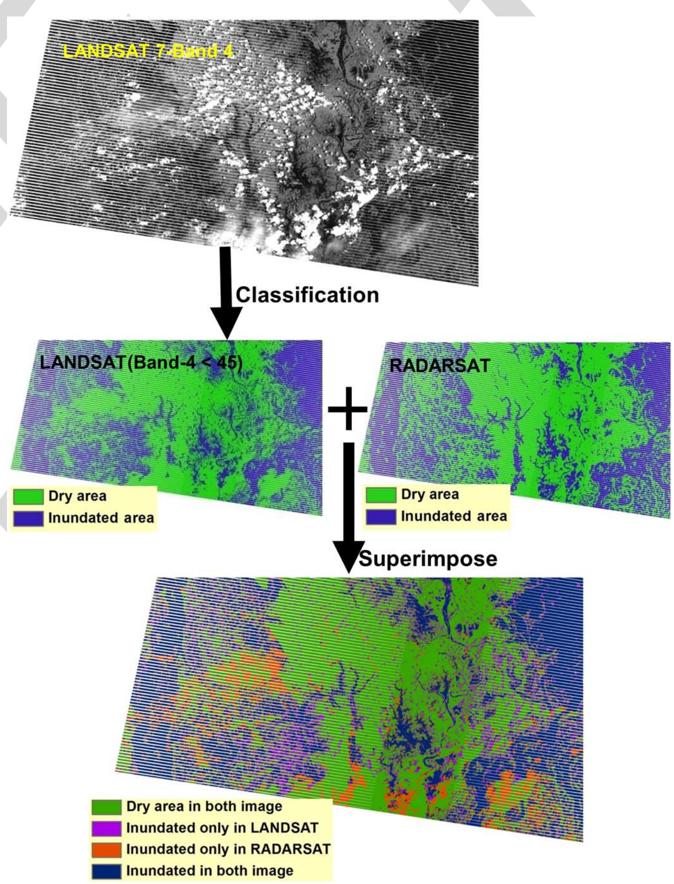

Fig. 3. Classification of LANDSAT-7 (band 4) image and comparison with RADARSAT.

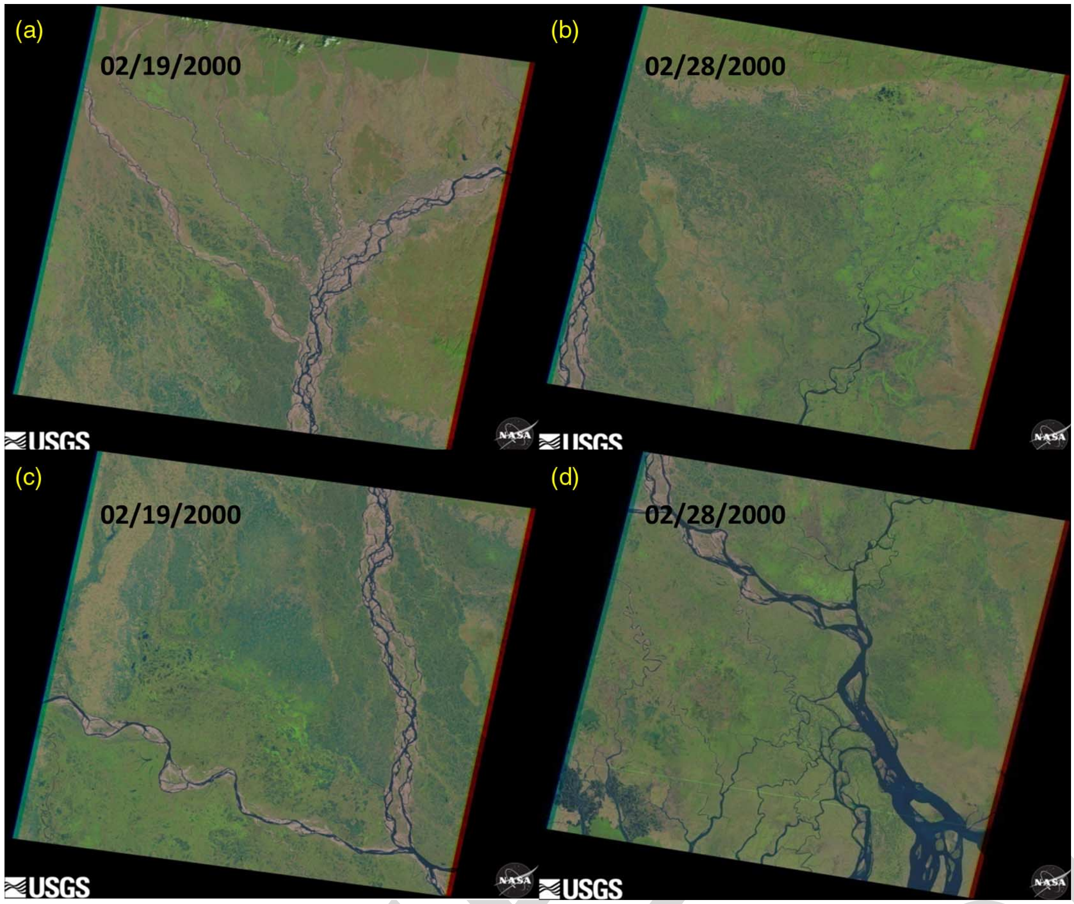

Fig. 4. LANDSAT-7 imagery used for Land–Water classification for the extraction of elevation of water pixels in Bangladesh Delta from SRTM data on February 20, 2000. (Source: USGS).

1) If the SRTM elevation data exhibit quantifiable skill in estimating the discharge according to the Manning's approach at a particular river section or reach, SWOT-era elevation data should have similar or higher skill. This is because the elevation measurements during the SWOT era are expected to be more accurate, more precise, and have a smaller native resolution by an order. In ours words, this can be phrased as, *if it works for SRTM elevation data, then it must work equally well or better for SWOT-era elevation data.* We argue that this knowledge of the circumstances for which discharge estimation is conclusively effective for SRTM data is the logical first step to push the envelope of accuracy for SWOT-era discharge algorithms.
2) Given the coarser resolution and larger uncertainty associated, the performance of SRTM elevation data-based discharge estimation is neither a necessary nor a sufficient condition for identifying the circumstances for which SWOT-era elevation data can be equally ineffective. In our words, this can be phrased as, *if SRTM elevation data does not work conclusively for a given case, one cannot make the same claim about SWOT-era elevation data until SWOT data is actually available.*
Q2 3) Given that observed discharge and water level data are not sampled (in space and time) frequently enough and are also sparsely distributed for a river network (including the Bangladesh Delta), derived discharge estimates and water level dynamics from an accurately calibrated hydrodynamic (HD) model are the acceptable candidates for benchmarking the spaceborne technique of discharge estimation.

This study is organized as follows. Section II provides a summary of the study region (river network) and HD model used. Section III elaborates the Manning's slope-area method of discharge estimation using spaceborne observables from SRTM. Section IV describes the uncertainty assessment of estimated discharge for various rivers followed by Section V (discussion) on ways to reduce uncertainty. Finally, Section VI addresses key conclusions and the likely way forward in advancing spaceborne discharge estimation.

II. The HD Model

An HD model was used to estimate the water level and discharge dynamics at closely spaced locations along a channel in the vastly intricate river network of Bangladesh. The key motivation that drove the building of this model was the absence of direct measurement of river stage and rated discharge along most river reaches of Bangladesh. The Hydrologic Engineering Centers River Analysis System (HEC-RAS) was used as the HD model by building on an earlier work of [29]. HEC-RAS is a one-dimensional (1-D) HD model which can simulate natural or

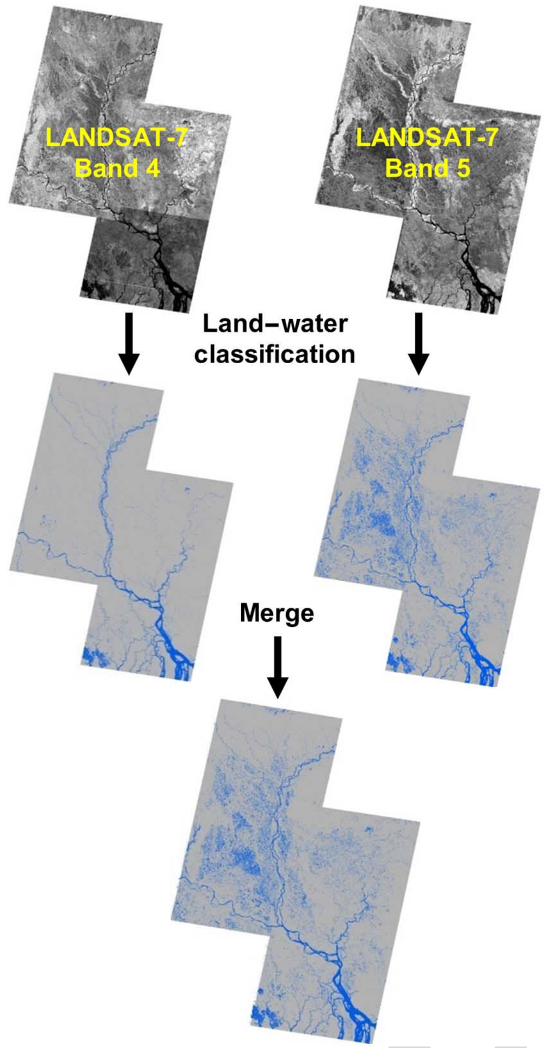

Fig. 5. Land–Water classification of LANDSAT imagery for the extraction of water elevations from SRTM data during February 20, 2000 in Bangladesh.

designed open channel network. It can simulate both steady and unsteady flow conditions. The steady flow simulation is based on 1-D energy equation. Here, Manning's equation is used to calculate the energy loss. HEC-RAS can generate flow and stage hydrographs at each cross section in unsteady flow condition. An earlier setup of HEC-RAS model comprising only three major rivers (Ganges, Brahmaputra, and Meghna) [29] was updated to include the numerous (and smaller dendritic) rivers (Fig. 1). For further details on the HEC-RAS setup, the reader is referred to [29].

A total of 124 rivers with over 2200 river bathymetric cross sections were used to create a comprehensive HEC-RAS model setup (Fig. 1). This updated setup has a total of 56 boundaries (48 upstream and 8 downstream). The setup is as stable "as is" during the Monsoon period. During the dry period of the year (October to May), the ephemeral streams, which become dry, require to be switched off to achieve numerical stability in the unsteady simulations. The calibration period for the model covered 2000–2002 (i.e., 3 years). Fig. 1 provides a summary of the calibrated and acceptable water level simulations during this period that are compared against observations. The RMSE of the

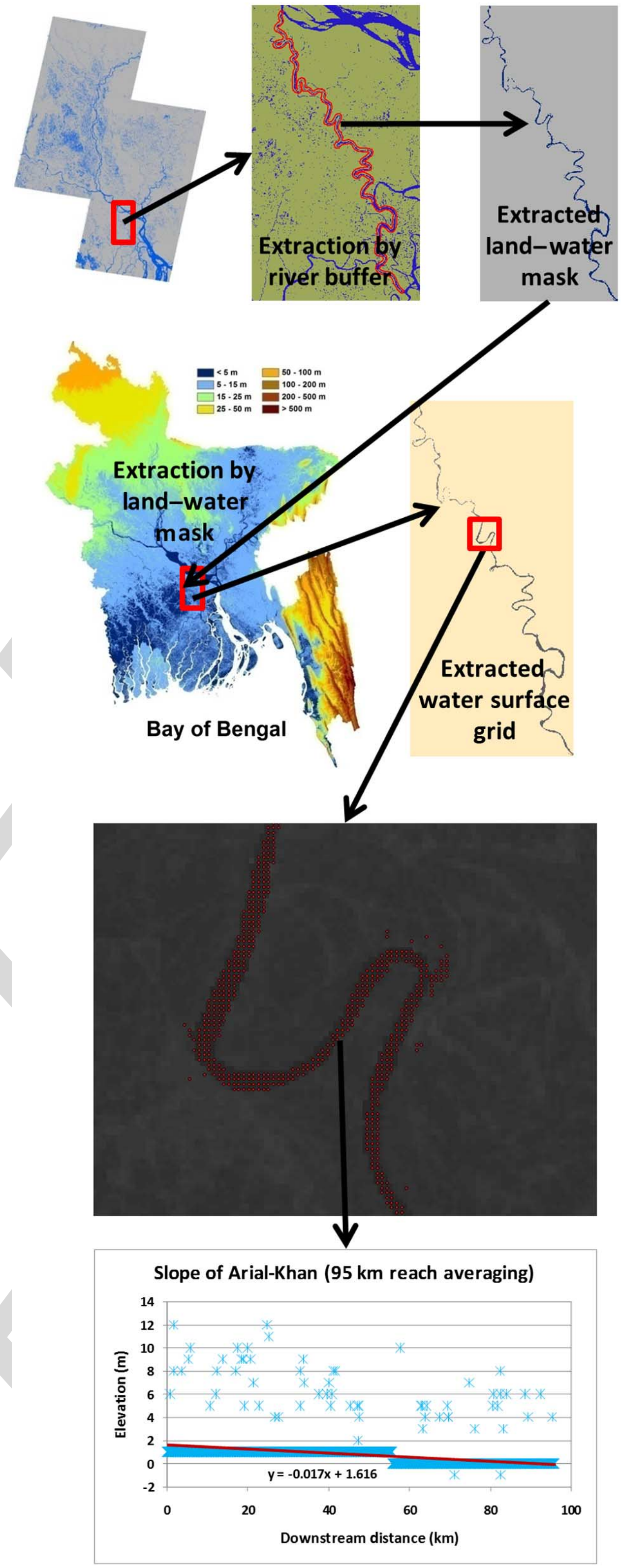

Fig. 6. Extraction of water elevation for the river Arial Khan from SRTM data and LANDSAT-classified land–water mask.

calibrated water level with observed water level ranged from 0.45 to 1.33 m. Fig. 1 indicates that the calibrated model is quite satisfactory during the dry period for use as a reference for water level dynamics along the river reaches.

III. Discharge Estimation From Satellite-Derived Elevation Data

A. General Methodology

Most of the studies using SRTM data to estimate discharge are performed with the Manning's approach (e.g., [15] and [34]). This technique of discharge estimation is based on the Manning's equation. The Manning's equation can be rearranged as follows considering that the flow is uniform, so that the friction slope S_f can be replaced by surface water slope S_o:

$$Q = \frac{1}{n} AR^{2/3} (\partial h/\partial x)^{1/2} \tag{1}$$

where n is Manning's roughness parameter, A is the cross-sectional area of flow, R is the hydraulic radius, and $\partial h/\partial x$ is the surface water slope. Here, stage and slope can be determined using SRTM data. If the *in situ* section data are available, cross-sectional area and hydraulic radius are also derivable.

SRTM data provide water surface elevation data for water bodies and rivers alongside land surface elevation. To extract the water surface elevation data to determine the stage and slope from SRTM data, a land–water mask is needed as the simplest methodology. So the steps to determine the spaceborne discharge using the Manning's approach with *in situ* bathymetry are: 1) creation of a land–water classification mask; 2) extraction of water surface elevation from SRTM data using the mask to determine the slope and water level; 3) calculation of cross-sectional area and hydraulic radius; and 4) applying Manning's equation to determine discharge. A flowchart of these steps to discharge estimation is provided in Fig. 2.

B. Classification of Land–Water Mask

In this study, water bodies were classified from available LANDSAT image using an unsupervised process reported in [21]. According to [21], water can be classified from land using the following simple rule of using bands 4 and 5 imagery of the Thematic Mapper (TM) sensor of LANDSAT:

Band 4 $(0.76 - 0.90\ \mu\text{m}) < 45$ value of digital image [= water]
Band 5 $(1.55 - 1.75\ \mu\text{m}) < 35$ value of digital image [= water].

Because the band 4 of ETM+ and TM uses same wavelength range while band 5 uses almost same wavelength range to take images, the unsupervised rule suggested by [21] for Landsat-TM imagery is also applicable for Landsat-ETM+ imagery. The quality of the land–water classification from LANDSAT image was verified by an independent SAR image of water bodies from RADARSAT [14], which is immune to cloud cover problems. For verification of land–water classification from LANDSAT image, a classified RADARSAT image of the study area was collected for August 3, 2007. The nearest LANDSAT-7 image (August 10, 2007) corresponding to the RADARSAT image had 17% cloud cover. Fig. 3 shows that the unsupervised scheme used for LANDSAT image classification into water and non-water pixels yielded 80% of the pixels correctly classified even with a fairly high cloud coverage (of 17%).

For extracting the water level data from SRTM, LANDSAT-7 imagery that was as close as possible to the SRTM overpass (February 20, 2000) was used. There are four such LANDSAT scenes that are available near February 20 (on February 19 and 28, 2000) with fairly low cloud cover (less than 10%; Fig. 4). All four images were classified as water and land and merged to create a mosaic over Bangladesh river networks (see Fig. 5) using the simple rule suggest by [21].

TABLE I
General Characteristics of Study Reaches of Rivers

River name	Study reach length (km)	Average top width (from LANDSAT image) (m)	Location in Bangladesh
Atrai	150	66	North-West
Baulai	92	170	North-East
Mohananda	70	171	North-West
Lakhya	112.5	182	North-Central
Arial-Khan	100	266	South-West
Ganges	124	1095	Major-River

C. Estimation of Water Elevation and Slope

The water surface elevation data of February 20, 2000 from SRTM data were extracted using LANDSAT water–land classified image and a GIS technique as follows. To simplify the extraction process, a line shapefile of the target river reach was used. Using this line shape, a buffer polygon of the river was created to extract only the river area. The buffer width was broad enough to cover the maximum width of a river reach and include the water areas of a river. The water surface elevation grid of the target river reach from SRTM data was extracted using the land–water mask of the reach. The extracted water surface elevation grid was then converted into point shapefile with grid values. Chainage (i.e., distance from upstream along river centerline) of each cell was calculated along the river. The slope was then determined from the relationship between the water surface elevation change and the horizontal distance of cells from the upstream end of the river. An example of water elevation extraction and slope calculation for the Arial Khan River (see Fig. 1 for its location) is shown in Fig. 6.

D. Estimation of Discharge

The water level at a particular river cross section was derived from the regression equation of derived slope from SRTM elevation data. Another set of discharge was estimated using the water level directly extracted from SRTM data at *in situ* section's location. There are two approaches to estimate discharge that were followed, with the former approach (using slope information to derive water elevation) being used in the hope that it would make the discharge estimates less sensitive to the noise in SRTM elevation data. The datum of SRTM-derived water elevation is an ellipsoid. But the datum of the available *in situ* cross sections/bathymetry is called "mPWD" and is set by the public work department (PWD) of the country. Thus, the SRTM-derived water level data were adjusted to the mPWD datum. The area and wetted perimeter of the available *in situ* cross section were calculated using simple geometric calculations. The

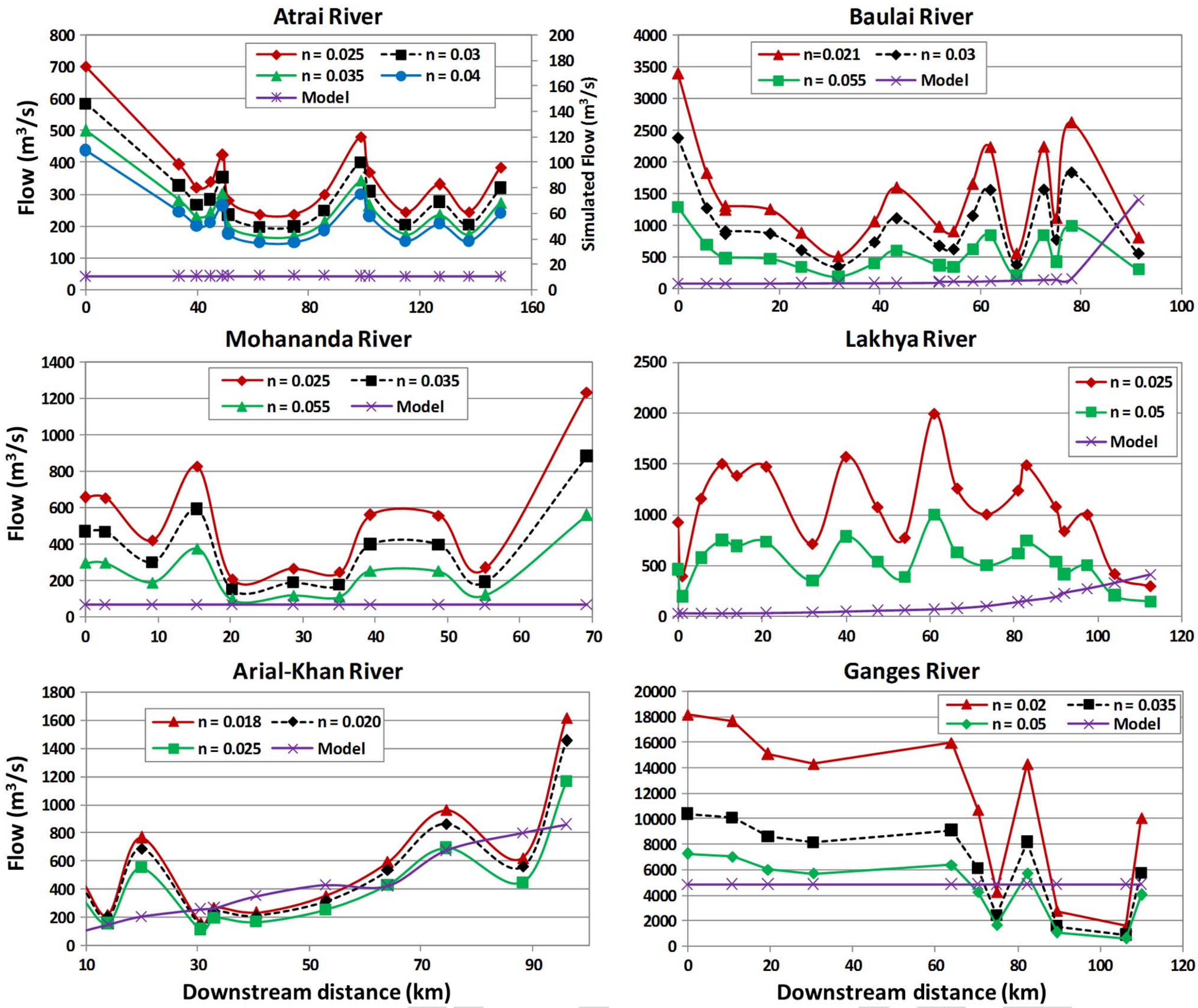

Fig. 7. Estimated discharge at study reaches with Manning's approach using minimum SRTM water surface elevation for different Manning's n.

hydraulic radius was derived from the area and wetted perimeter of the cross section. The derived area (A), hydraulic radius (R), water surface slope ($\partial h/\partial x$), and approximated Manning's roughness (n) were used to determine the discharge through Manning's equation (1).

IV. Uncertainty Analysis

A. Error Metrics for Uncertainty Analysis

The uncertainty of the spaceborne estimated discharge with the calibrated model-simulated discharge was calculated by the coefficient of variation of the root-mean-square error of *CV (RMSE)*, which can be defined by the following equation:

$$CV(RMSE) = \frac{RMSE}{\overline{Q}} \tag{2}$$

where $RMSE$ is the root-mean-square error of the estimated discharge relative to the model (HEC-RAS) discharge and $\overline{Q}$ is the average of reference (i.e., HD modeled) discharge. Root-mean-square error of the estimated discharge was determined using

$$RMSE = \sqrt{\frac{\sum_{t=1}^{n}\left(Q_{e,t} - Q_{r,t}\right)^2}{n}} \tag{3}$$

where $Q_{e,t}$ represents estimated discharge, $Q_{r,t}$ is the reference discharge at same location, and n is the number of total cross sections, where discharge were estimated.

CV(RMSE) indicates the variation of estimated discharge relative to the reference (i.e., HEC-RAS model output in this case). In other words, a low *CV* smaller than 1 indicates that the error variability is an order smaller than the natural variability of (measured) flow and thus quite reliable.

Six rivers were selected to carry out the accuracy analysis of discharge estimation (Fig. 1). The reaches are selected to afford variability in width, bed slope, and topographic regions (flat versus mountainous) of Bangladesh. The selected reaches, in order of increasing river width, were: Atrai, Baulai, Mohananda,

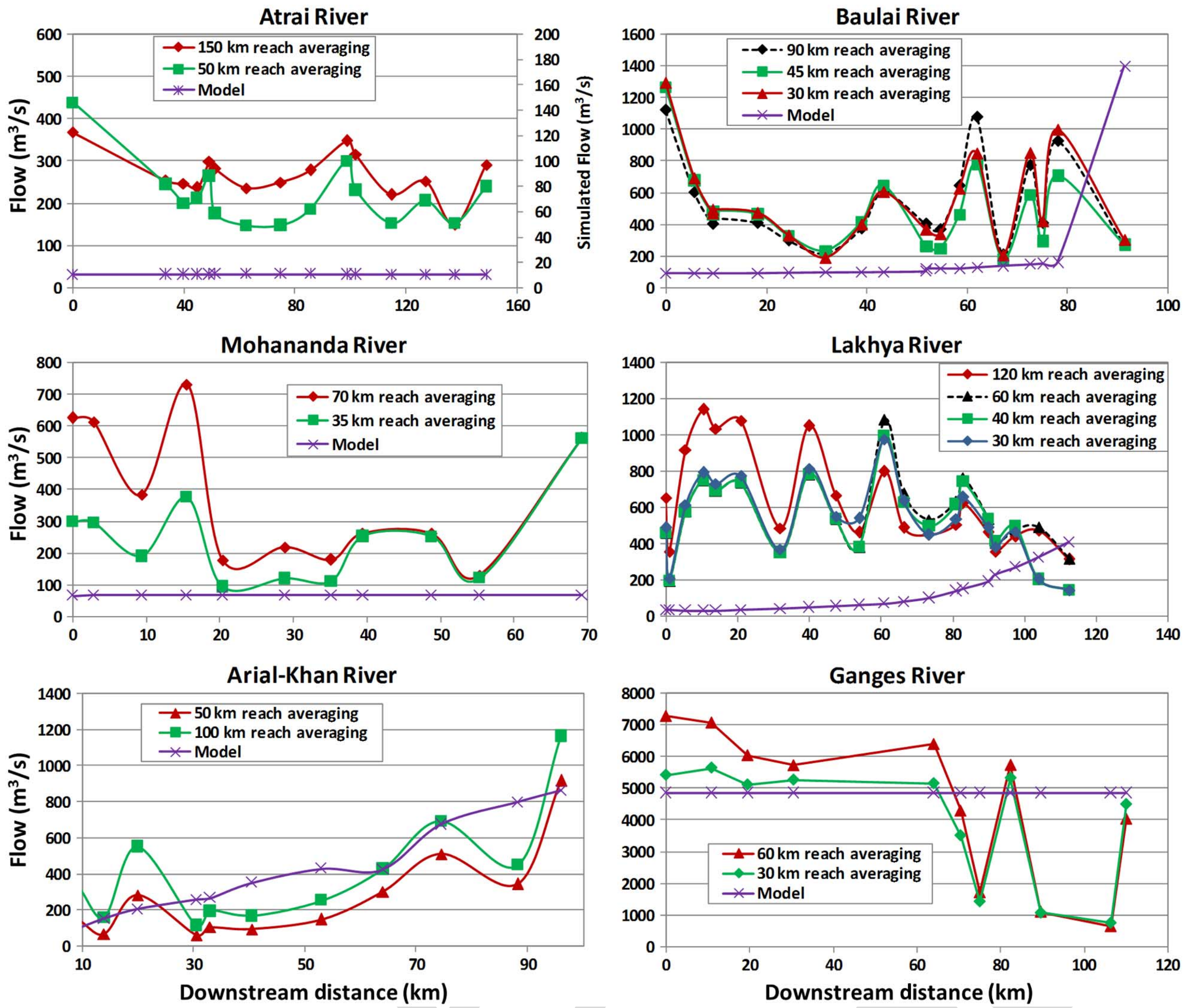

Fig. 8. Estimated discharge with best-fitted Manning's n using minimum SRTM water surface elevation for different reach averaging length. "Model" refers to discharge estimated by HEC RAS HD model.

Lakshya, Arial Khan, and Ganges. General characteristics of the selected river reaches are shown in Table I.

B. SRTM-based Discharge Estimation of Rivers

Discharge was estimated for all six study reaches with varying Manning's n (Fig. 7). In this scenario, water level at each *in situ* cross section was determined using the first-order polynomial regression equation of the derived slope. Fig. 7 shows that the accuracy of estimated discharge generally increases with the use of higher assumed Manning's n. The estimated discharge of the Ganges and the Arial Khan rivers were closest to the reference (model- HEC RAS)-simulated discharge. Both rivers are wider than 250 m. The Atrai River, which was the narrowest river of the six, yielded the highest uncertainty in discharge estimation. Calculated discharge at each section of the Atrai River is found to be at least one order higher than the reference discharge from the HD model, indicating that the Manning's approach using SRTM data is inappropriate without further corrections.

Next, the best-fitted Manning's n, among the evaluated Manning's n, was selected for the next set of analyses. The discharge was estimated for different reach averaging lengths with the best-fitted Manning's n (shown in Fig. 8). Two reach averaging lengths of each river were selected based on available total length of the river reach and the slope of the river. The accuracy of the estimated discharge generally seemed insensitive, particularly for the wider rivers such as Ganges and Arial Khan. However, for Baulai and Lakshya rivers, where discharge was estimated for more than two reach-averaged lengths, there appeared to be an "optimal" reach averaging length. For Baulai and Lakshya rivers, this optimal length appears to be about 40 km. A point to note is that the discharges estimated herein used only the reach-averaged slope, whereas all other hydraulic parameters were derived for each *in situ* cross section. Later in Section V, we revisit this issue by performing a truly reach-averaged discharge estimation using reach averaging for all hydraulic parameters.

A sensitivity analysis was also done to compare the discharge estimated using water level extracted by the two contrasting

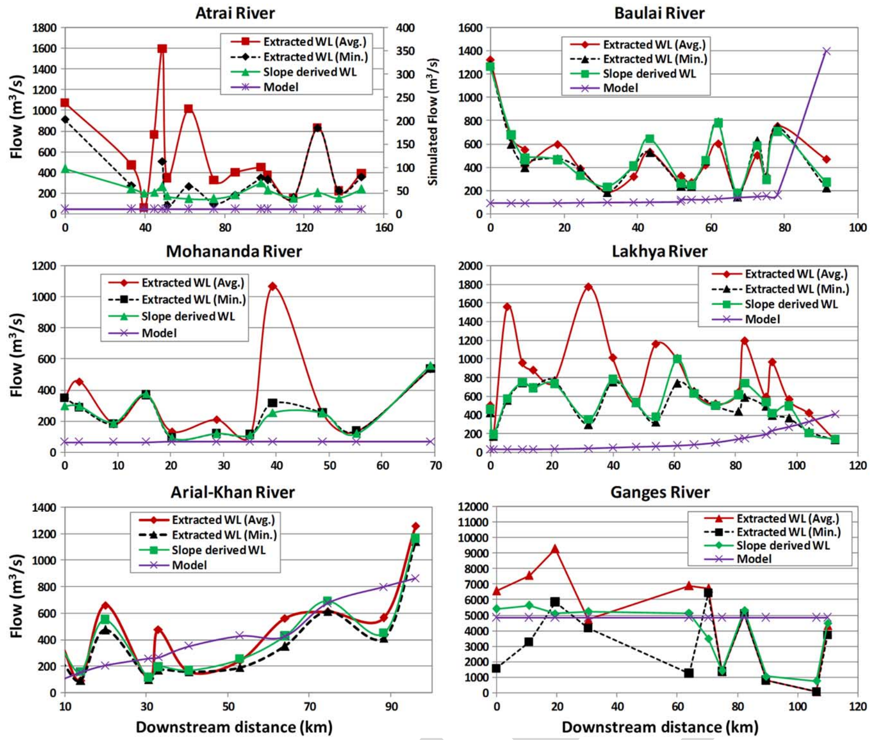

F9:1 Fig. 9. Estimated discharge with optimized reach-averaged length and best-fitted Manning's n for different approaches of water level acquired. "Model" refers to flow
F9:2 simulated by HEC RAS HD model.

TABLE II

T2:1 CV(RMSE) of Spaceborne Estimated Discharge Compare to Simulated Discharge With Different Average Widths,
T2:2 Average Water Surface Slope, and Average Bed Slope

River name	Reach (km)	Avg. width from LANDSAT (m)	Avg. slope (cm/km)	Bed slope (cm/km)	CV (RMSE)	Acceptable (Y if CV< 1; N if CV >1)
Atrai	0–50	90	–7.0	–2.2	21.96	N
Atrai	50–100	64	–4.0	–10.3	16.96	N
Atrai	100–150	44	–2.3	–1.6	17.71	N
Atrai	0–150	66	–4.0	–6.8	23.92	N
Arial-Khan	0–100	266	–1.9	–8.1	0.47	Y
Arial-Khan	0–50	264	–0.3	–4.6	0.69	Y
Arial-Khan	50–100	268	–0.6	–4.2	0.36	Y
Lakhya	0–112.5	182	–5.6	0.7	5.12	N
Lakhya	0–61	152	–2.8	–2.4	12.65	N
Lakhya	61–98	207	–6.9	1.2	3.26	N
Lakhya	98–112.5	239	–1.6	–11.8	0.55	N
Baulai	0–92	170	–2.1	–5.2	3.00	N
Baulai	0–30	125	–5.1	8.6	6.58	N
Baulai	30–60	180	–4.6	1.4	3.04	N
Baulai	60–92	203	–4.6	10.2	1.98	N
Mohananda	0–70	171	–3.0	4.0	5.46	N
Mohananda	0–38	179	–0.8	12.7	2.63	N
Mohananda	38–70	157	–3.0	–3.5	4.08	N
Ganges	0–31	1051	–5.3	0.0	0.11	Y
Ganges	62.5–93	1207	–11.7	–21.0	0.49	Y
Ganges	93.5–124	906	–16.9	–361.6	0.60	Y

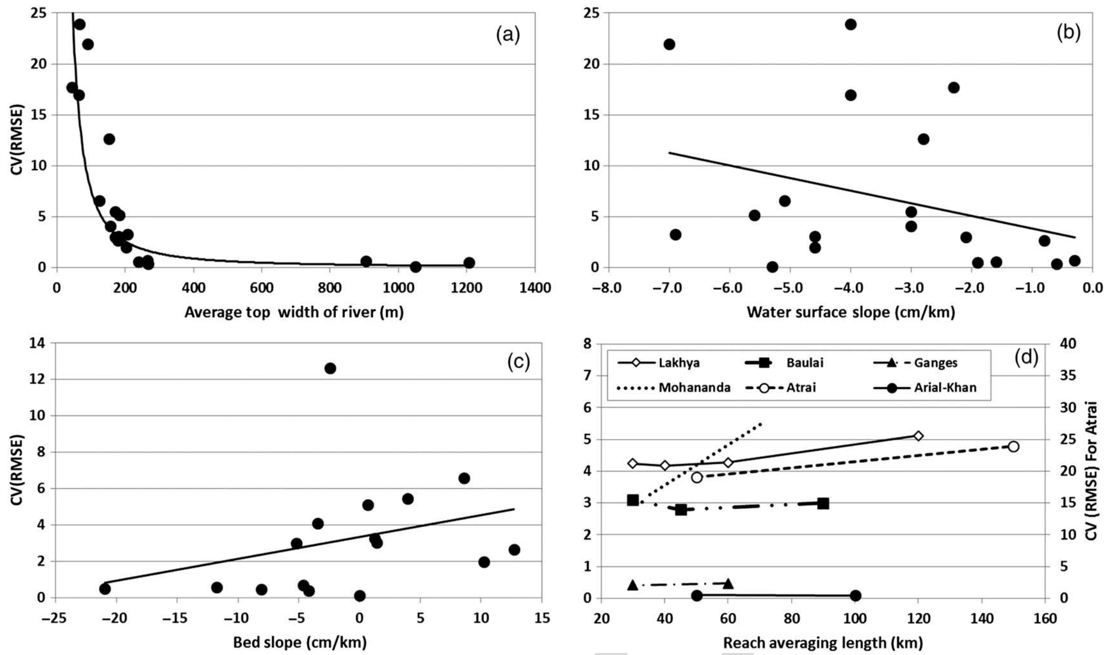

Fig. 10. Accuracy of discharge estimation with (a) change of river top width (classified from LANDSAT); (b) change of average water surface slope; (c) change of average bed slope; and (d) change of reach averaging length.

TABLE III
CV(RMSE) of Spaceborne Estimated Discharge Compare to Simulated Discharge With Different Reach Averaging Lengths

River name	Reach averaging length (km)	CV(RMSE)	Acceptable (Y if CV< 1; N if CV> 1)
Atrai	50	19.02	N
Atrai	150	23.92	N
Arial-Khan	100	0.47	Y
Arial-Khan	50	0.49	Y
Lakhya	30	4.24	N
Lakhya	40	4.17	N
Lakhya	60	4.27	N
Lakhya	120	5.12	N
Baulai	90	3.00	N
Baulai	45	2.80	N
Baulai	30	3.10	N
Mohananda	70	5.46	N
Mohananda	35	3.24	N
Ganges	60	0.47	Y
Ganges	30	0.42	Y

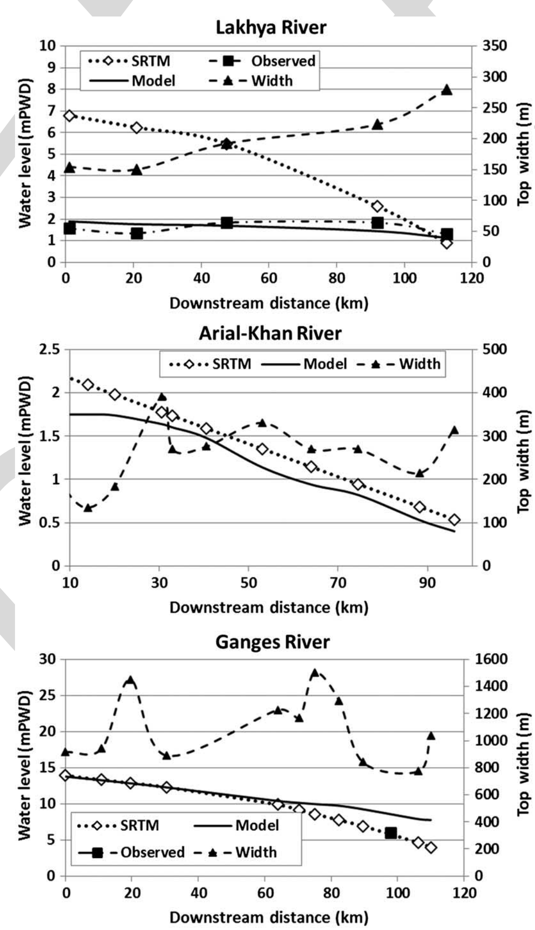

Fig. 11. Comparisons of SRTM-derived water level with simulated and observed water level along with change of river width. Here, width is computed from classified LANDSAT image.

approaches mentioned earlier (Fig. 9). The first approach of water level derivation was simply to use the regression equation (first order polynomial) of water slope. For this approach, the minimum water level was estimated along each river reach, and river cross section was used. The second approach was directly

TABLE IV
DERIVED WATER LEVEL USING DIFFERENT APPROACHES IN THREE RIVERS (ALL WATER LEVELS ARE SHOWN IN METERS ABOVE THE PWD DATUM OF BANGLADESH)

River	Chainage (km)	WL climatology of February	WL simulated by HD model	Slope derived WL from SRTM	Adjusted slope derived WL from SRTM	Minimum WL from SRTM	Adjusted minimum WL from SRTM
Lakhya	21	1.16	1.76	6.23	2.24	6.46	2.70
Lakhya	112.5	1.19	1.13	0.89	1.30	0.46	0.75
Baulai	67.2	1.35	1.55	3.26	1.32	3.46	1.41
Lakhya	0	1.46	1.91	6.81	2.54	6.46	2.70
Lakhya	54	1.53	1.69	5.30	1.85	5.46	2.20
Lakhya	92	1.56	1.45	2.58	1.25	2.46	1.12
Baulai	39	1.75	1.54	4.39	1.56	4.46	1.77
Atrai	197.75	3.81	3.77	5.89	2.09	5.46	2.20
Atrai	85.5	8.99	8.71	13.42	8.57	13.46	8.16
Atrai	33.5	13.06	13.45	16.16	12.49	16.46	11.55
Atrai	0	16.19	13.8	18.50	16.53	20.46	17.05

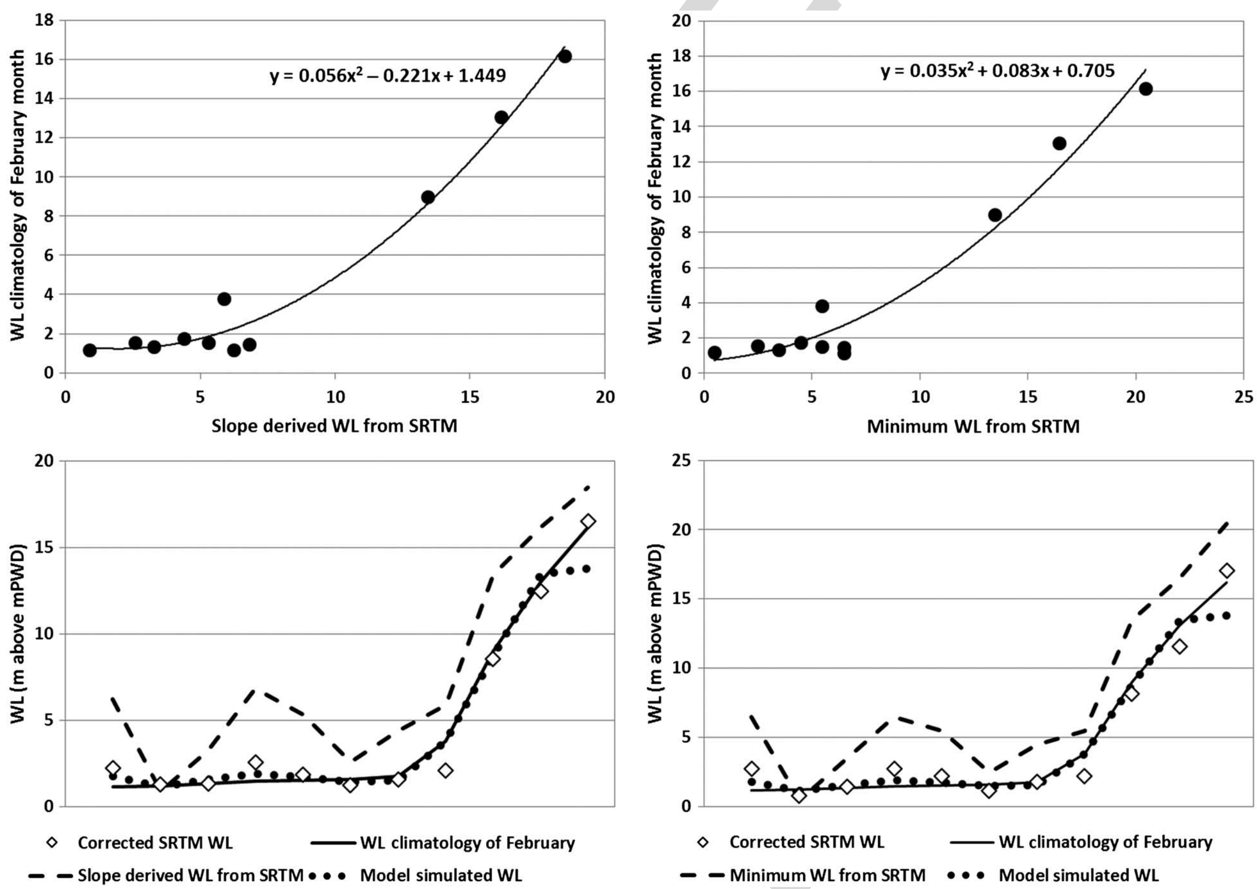

Fig. 12. Upper panel—correlation between water level climatology and water level from SRTM data (left is for slope-derived WL and right is for directly extracted minimum WL). Lower panel—adjusted SRTM water level using flow climatology (left is for slope-derived WL and right is for directly extracted minimum WL).

extracted water level from SRTM data at *in situ* section location. In this case, discharge was determined using both minimum and average water level at each cross section of reaches as suggested in [17]. Fig. 9 shows that the discharge calculations using the slope-derived water level are very similar to that obtained through minimum water level directly acquired from SRTM data. For Atrai and Ganges rivers, the slope-derived water level yields marginally better accuracy than that using the directly estimated minimum water level.

C. Assessment of Uncertainty

Accuracy of satellite-based discharge estimation was calculated by *CV(RMSE)* (2). Calculated values of *CV(RMSE)* for

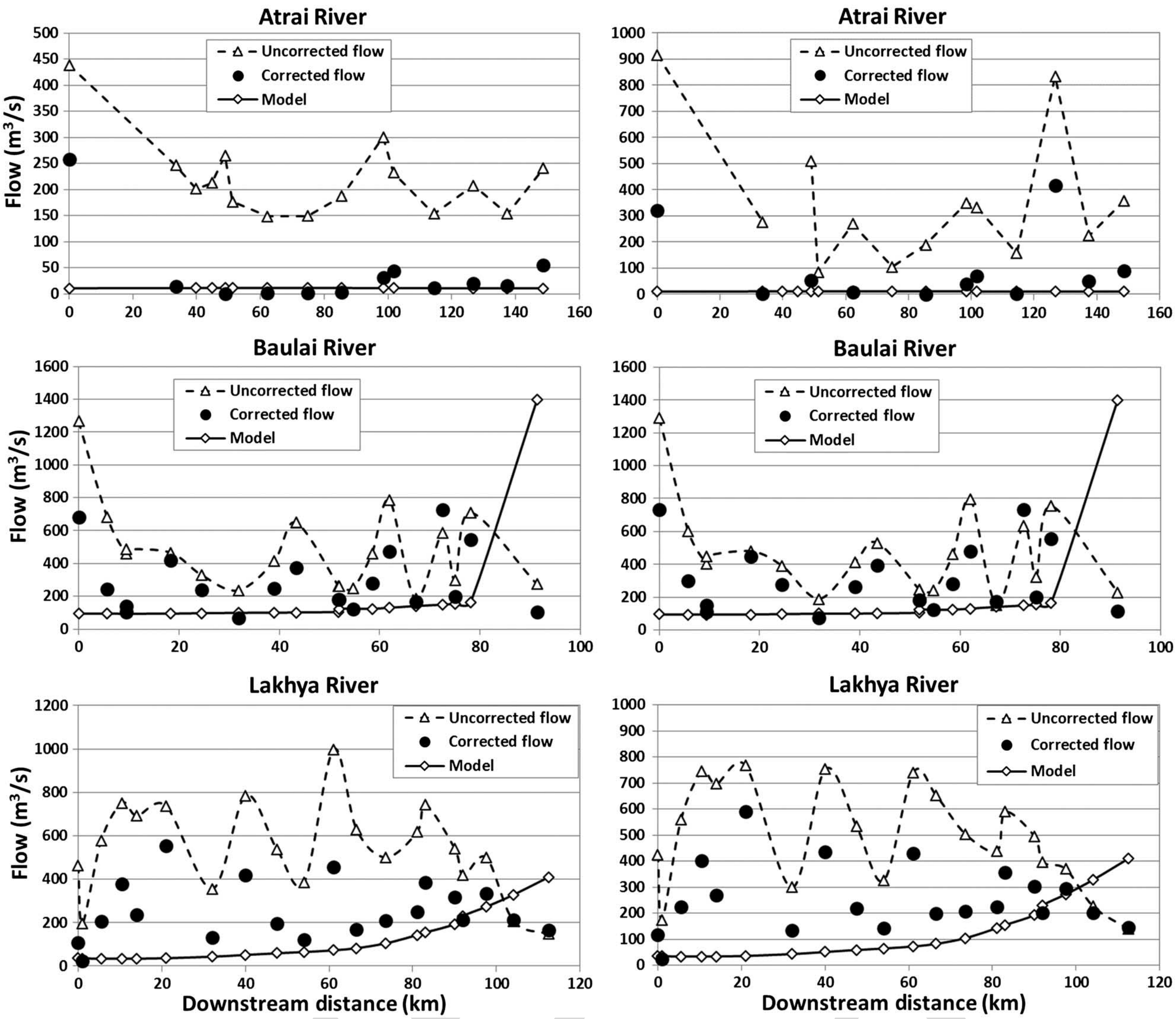

Fig. 13. Comparison between discharge estimation using climatology-adjusted SRTM water level and unadjusted SRTM-derived water level along with model (HD)-simulated flow (left panel for slope-derived water level and right panel from directly extracted minimum water level from SRTM).

TABLE V
COMPARISON OF CV(RMSE) BETWEEN DISCHARGE DERIVED FROM CLIMATOLOGY-ADJUSTED AND UNADJUSTED SRTM WATER LEVEL

River name	Reach averaging length (km)	Manning's n	CV(RMSE)			
			Slope derived WL		Minimum WL	
			Unadjusted	Adjusted	Unadjusted	Adjusted
Atrai	50	0.04	20.18	6.16	38.57	14.44
Baulai	45	1.19	2.80	2.13	2.80	2.17
Lakhya	40	1.35	4.17	1.80	3.79	1.88

different rivers with varying average width (i.e., average top width from classified LANDSAT image), water surface slopes, and bed slopes are shown in Table II. A point to note herein is that negative bed slope means a downward slope along the downstream direction downstream and positive bed slope means upward slope to downstream.

The plots of *CV(RMSE)* versus average width, average slope, average bed slope, and reach averaging length are shown in Fig. 10. The *CV(RMSE)* versus average width plot [Fig. 10(a)] appears to follow a logarithmic function with *CV* decaying rapidly at river widths larger than 250 m. In relative terms, this equates to about three times the native spatial resolution of the spaceborne elevation data. While this rule cannot and should not be generalized for the SWOT-era elevation data, given the contrasting scale, accuracy, and precision, it is fair to claim that SWOT data should be able to improve on this rule and yield more accurate discharge estimates for rivers that are narrower than three times the native resolution of SWOT elevation data. An issue to keep in mind is the science requirement of the SWOT mission (at the time of writing this manuscript) is that height accuracy (sigma) will be 10 cm or lower when averaged over an area that is $1\ \mathrm{km}^2$. For a river that is 100 m wide, this translates to a reach length of 10 km, and seems quite promising during the SWOT era for the narrow rivers (width $<270\ \mathrm{m}$) that were found not as promising using SRTM data.

For *CV(RMSE)* versus average surface water slope plot [Fig. 10(b)], two extreme water surface slopes of the Ganges river (11.7 and 16.9 cm/km) were excluded as outlier. The plot shows that the *CV(RMSE)* generally follows a weakly decreasing trend with decreasing surface water slope and in general the trend is rather inconclusive (note: negative slope means the slope is downhill). The plot of *CV(RMSE)* versus average bed slope shows a similarly weak but increasing trend of *CV(RMSE)* with decreasing bed slope (compared to water surface slope) [Fig. 10(c)].

Another accuracy analysis was performed with reach averaging length. Table III shows the *CV(RMSE)* for different reach averaging lengths in different rivers. The sensitivity to accuracy of discharge estimation with change of reach averaging length is shown in Fig. 10(d). The Baulai and the Lakshya rivers, where more than two reach averaging lengths were used to determine the discharge, showed an optimal reach averaging length. Thus, too much or too little reach averaging length can increase uncertainty in discharge estimation for such rivers with medium width (between 100 and 250 m).

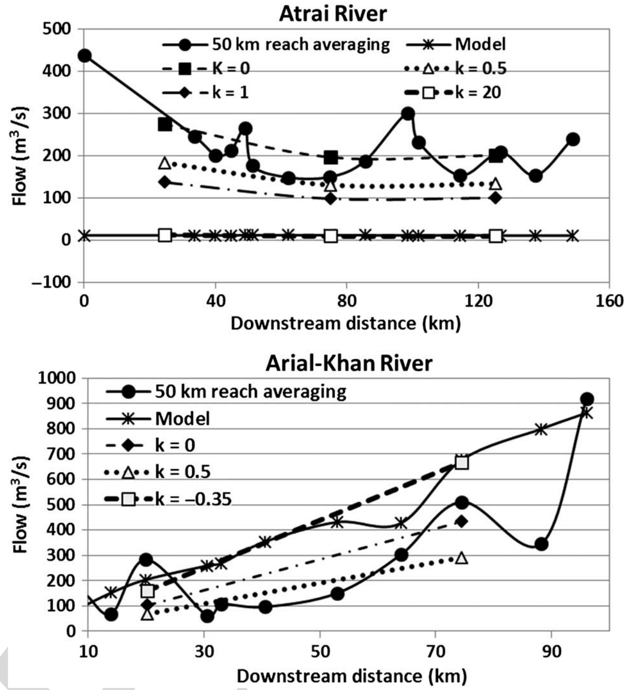

Fig. 14. Reach-averaged discharge using reach-averaged hydraulic parameters and correction factor k (4). Upper panel for Atrai River (width less than 100 m) and lower panel for Arial Khan river (width usually larger than 250 m).

V. Reducing Uncertainty of Discharge Estimation

A. Key Sources of Uncertainty

Analysis according to [10] shows that uncertainty can arise from change in cross-sectional area (∂A), width (W), slope (S_w), cross-sectional area at lowest stage, and Manning's n (A_o and n). A study reported in [18] analyzed the Ohio River and showed that 95% uncertainty in discharge calculation occurred due to roughness coefficient and friction slope. In our study, *in situ* bathymetry data were used. Therefore, it is directly measurable and uncertainty from should be less significant. Furthermore, optimal Manning's n was used to find the best-fit with observed discharge to reduce uncertainty from Manning's n (Fig. 7). Finally, discharge was estimated for various slopes estimated from reach-averaged lengths (Fig. 8) to minimize the uncertainty from slope. Thus, the major source of uncertainty is likely to be contributed by the error in estimation of cross-sectional area and hydraulic radius due to erroneous estimation of river stage from SRTM data.

To verify whether the erroneous estimation of river stage is the key source of uncertainty, Fig. 11 shows the comparison of extracted water level from SRTM with HD model simulated and observed water level measurement for Lakshya River. In this river reach, a large error in elevation measurement occurred at upstream locations, where top width of the river (from LANDSAT image) was about 150 m. This top width of the river is seen to increase along the downstream direction, as discharge estimation error decreases. Another example of Arial Khan River (Fig. 11) shows that the error in stage measurement is relatively large at upstream locations. The error becomes minimum and almost constant beyond a 250-m river top width. The Ganges River is the widest river among all the study reaches and width is considerably higher than 250 m at each section. Accuracy of water level estimation from SRTM was significantly higher and closer to the observed data for the Ganges River (see Fig. 11).

From Fig. 11, it is clear that the accuracy of water level measurement using SRTM data depends mostly on the width of the river that consequently dictates the likelihood of contamination by land elevation data and overestimation of section factor and discharge. The accuracy is relatively high and almost constant for river width larger than 250 m, which is almost equal to width of three times the native spatial resolution (90 m) of SRTM data (noted earlier in Section IV).

B. Using Flow Climatology to Reduce Estimation Uncertainty

A statistical climatology-driven correction approach was applied to reduce the high levels of uncertainty that was found to occur in the narrower rivers. First, a simple regression analysis (mapping) was established between SRTM-derived water level and a 10-year climatology of water level for the month of February for the three rivers with width less than 270 m: Lakshya, Baulai, and Atrai. Here, a 10-year water level climatology was used instead of daily water level (for February 20, 2000) to correlate with SRTM data. Daily data may contain reading error, as it represent only a single measurement. Climatology is a long-time average of data where the RMSE is expected to minimize significantly.

In Table IV, water level climatology shows the daily average for the month of February over 10 years at each station. Both slope-derived (Table IV, column 5) and directly extracted

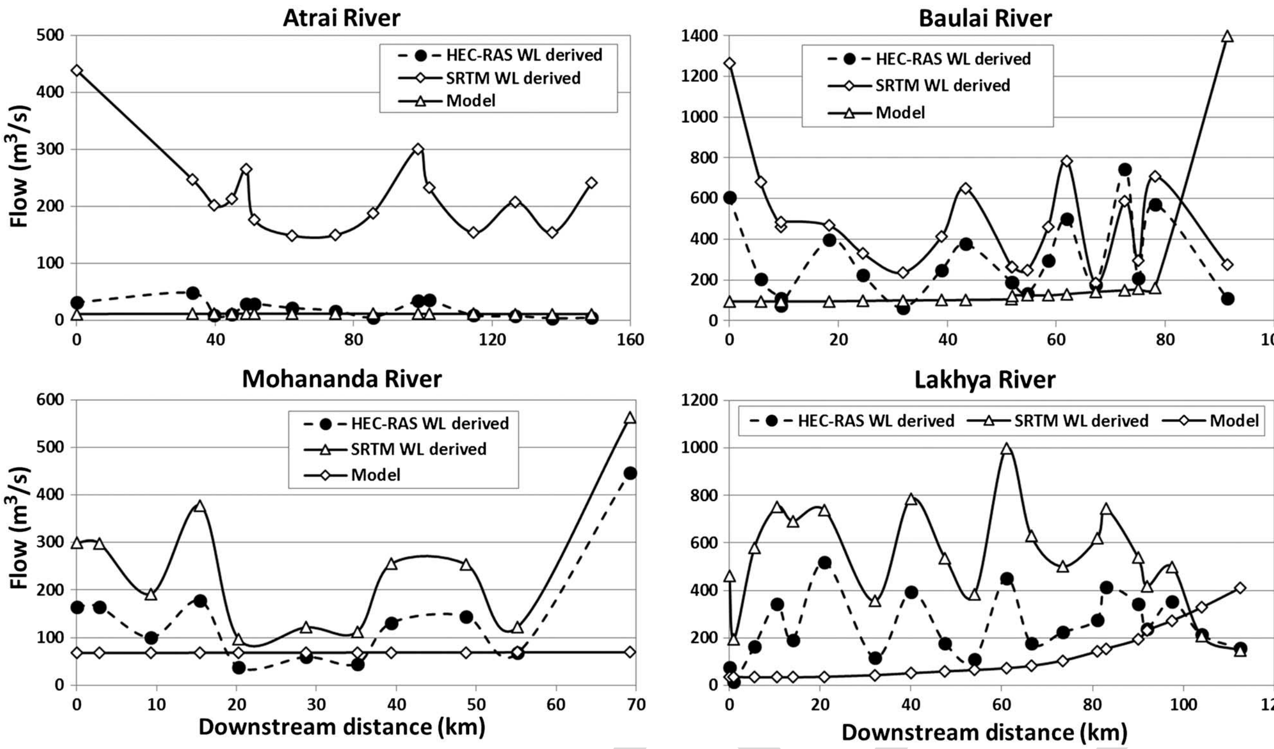

F15:1 Fig. 15. Inherent uncertainty of Manning's approach (i.e., model structural uncertainty) when there is no error assumed in slope or elevation.

T6:1 TABLE VI
CV(RMSE) of Discharge Estimation Using SRTM Water Level and HEC-RAS Water Level

River name	Reach (km)	Manning's n	Avg. width (m)	Avg. slope (cm/km)	Bed slope (cm/km)	CV (RMSE) for SRTM WL derived flow	CV (RMSE) for HEC-RAS WL derived flow
Atrai	0–50	0.04	90	–7.0	–2.2	21.96	1.82
Atrai	50–100	0.04	64	–4.0	–10.3	16.96	1.26
Atrai	100–150	0.04	44	–2.3	–1.6	17.71	1.10
Baulai	0–45	0.055	136	–4.9	–10.0	5.58	2.39
Baulai	45–92	0.055	200	–2.3	–10.3	1.86	1.86
Mohananda	0–38	0.055	179	–0.8	12.7	2.63	1.01
Mohananda	38–70	0.055	157	–3.0	–3.5	4.08	2.84
Lakhya	0–61	0.05	152	–2.8	–2.4	12.65	5.29
Lakhya	61–98	0.05	207	–6.9	1.2	3.26	1.20
Lakhya	98–112.5	0.05	239	–1.6	–11.8	0.55	0.53

minimum (Table IV, column 7) water level from SRTM data were correlated with observed water level climatology (Table IV, column 3). The observed climatology and SRTM water level correlation are found to follow a second-order polynomial trend. Fig. 12 (upper panel) shows the correlation and regression equation for both slope-derived and directly extracted SRTM water level. Using these regression equations, the SRTM water elevation data were "mapped" to the climatology (Table IV, column 6 and 8). Fig. 12 (lower panel) shows the impact of this climatology adjustment when compared to reference (HD model)-derived water level. Next, discharge was reestimated using the climatology-adjusted SRTM water level for both slope-derived and directly extracted elevation scenarios. Fig. 13 and Table V show the improvement in discharge estimation accuracy for the Atrai, Baulai, and Lakshya rivers using climatology-adjusted corrections. It is quite evident from the figure and table that the climatology-based adjustment of satellite elevation data can significantly enhance the skill of discharge estimates in rivers narrower than three times the native spatial resolution.

C. Using Correction Factor in Reach-Averaged Discharge to Reduce Uncertainty

As was noted earlier in Section IV, the discharges estimated up to this point used only the reach-averaged slope in the Manning's equation, while all other hydraulic parameters were derived as "point" values at each *in situ* cross section. Thus for two rivers of contrasting widths (Atrai and Arial Khan), discharge was reestimated using truly reach-averaged hydraulic parameters (area A and radius R) and assuming a correction factor k that is needed for adjustment (4)

$$Q = \frac{\overline{A}\,\overline{R}^{2/3}\overline{S}^{1/2}}{n(1+k)}. \tag{4}$$

For each river averaging length segment, the point-based calculations of area of flow and hydraulic radii were averaged along with reach-averaged slope. Fig. 14 shows the estimation of reach-averaged discharge for various arbitrary k factors for Atrai (upper panel) and Arial Khan rivers (lower panel). It is evident that an arbitrary and river-specific k factor can yield reach-averaged discharge that matches closely with model-derived discharge. However, the consistency of this correction factor for other times and diverse flow regimes remain untested due to SRTM sampling only for 1 day in February 20, 2000.

D. *Inherent Uncertainty of the Manning's Approach*

It is important at this stage, given the range of uncertainty in SRTM-derived discharge estimation that has been shown, to ask what could be the baseline or inherent uncertainty of the Manning's approach. The Manning's equation is essentially a grossly simplified form of the full HD flow equation, where it is assumed that the energy gradient line, the river bed and water surface are all parallel and thus the water surface slope is an acceptable proxy for driving discharge. Since we have treated HEC-RAS-derived water level as our reference, we, therefore, chose to recalculate the Manning's discharge using HEC-RAS-derived water level and compare it with that obtained from SRTM-derived water level. Fig. 15 and Table VI show that the inherent uncertainty of the Manning's approach can range from 10% to 30% depending on the river reach and flow conditions. This is an important issue to keep in mind as a key limitation of the Manning's approach when assessing the potential of satellite-based water elevation data that is expected from the SWOT mission. Other discharge algorithms beyond the Manning's approach should be considered when creating SWOT discharge products.

VI. Conclusion

This study was motivated by the need to understand the uncertainty of discharge estimation using the slope-area (Manning's equation) method using satellite interferometric elevation data. The study tried to contextualize the understanding as a function of river's geophysical characteristics (river width, reach length, and bed/water slope) of a riverine country in a humid deltaic environment (Bangladesh). The study also explored a pragmatic approach to uncertainty reduction using flow climatology. A high-resolution HD model was accurately calibrated to simulate water level and flow dynamics along the river reaches of the river network and serves as reference for comparison with satellite-based estimates. It was found that satellite interferometric (SRTM)-based discharge estimates yielded estimation error variance an order smaller than the natural flow variability only if the river width was at least three times larger the width of the native resolution of elevation data. It was also found that water level climatology can be useful in significantly reducing the estimation uncertainty for these narrow rivers. While reach averaging length appeared relatively insensitive to accuracy for wide rivers (width >1 km), a few rivers seemed to have an optimal length at which the highest accuracy is obtained. Finally, it was found that if reach-averaged hydraulic parameters (area, slope, and radius) are used for calculation of reach-averaged discharge, then the necessary linear (bias) correction factors needed are not only unique but also arbitrary for each river.

While the study findings are conditioned on the scale, accuracy, and precision aspects of SRTM data, the conclusions that emerge can provide guidance to the further development of discharge algorithms for the SWOT era. The typical 22-day (maximum) repeat sampling for the proposed mission at the planned 78° inclination will provide at least two observations in 3 weeks over the humid tropics and delta environments such as Bangladesh. Yet, when it comes to rigorous assessment of the potential of satellite remote sensing of fresh water fluxes, ungauged riverine deltas have remained a rather poorly studied region. This study has shown the scenarios for which SWOT-era elevation may be expected to provide skill in discharge estimation and perhaps with considerably lower uncertainty than that obtained using SRTM data. Furthermore, the study has shown that the use of water level climatology and correction factors have promise for improving the quality of discharge estimates.

A key limitation of the study, due to the nature of the SRTM, was the reliance on a single day (February 20, 2000) for assessing the uncertainty of satellite-based discharge estimation. A natural extension of this study is, therefore, to overcome this sampling limitation through the use of a simulator that can mimic SWOT-like interferograms, albeit with SWOT-like precision, orbit, sampling, and accuracy, from accurately measured water elevation maps. A first task for authors in the use of the SWOT simulator is to assess the minimum river top width for which reliable estimates of discharge can be obtained consistently during Monsoon and non-Monsoon seasons. Work is underway to use such a simulator and the findings will be reported in a forthcoming publication.

Acknowledgment

The Institute of Water Modeling, Dhaka, Bangladesh, is gratefully acknowledged for their generous support with data acquisition and hydrodynamic modeling as part of a 5-year memorandum of understanding with the Department of Civil and Environmental Engineering, University of Washington, Seattle, WA, USA. The authors also acknowledge the critique from the anonymous reviewers and the editor that helped improve the quality of the manuscript.

References

[1] D. E. Alsdorf, E. Rodriguez, and D. P. Lettenmaier, "Measuring surface water from space," *Rev. Geophys.*, vol. 45, no. 2, Jun. 2007.

[2] S. Biancamaria, F. Hossain, and D. P. Lettenmaier, "Forecasting transboundary river water elevations from space," *Geophys. Res. Lett.*, vol. 38, no. 11, Jun. 2011.

[3] C. M. Birkett, "The contribution of TOPEX/POSEIDON to the global monitoring of climatically sensitive lakes," *J. Geophys. Res.*, vol. 100, no. C12, pp. 179–204, Dec. 1995.

[4] G. R. Brakenridge, J. C. Knox, E. D. Paylor II, and F. J. Magilligan, "Radar remote sensing aids study of the great flood of 1993," *Eos Trans. AGU*, vol. 75, no. 45, pp. 521–527, Nov. 1994.

[5] G. R. Brakenridge, S. V. Nghiem, E. Anderson, and S. Chien, "Space-based measurement of river runoff," *Eos Trans. AGU*, vol. 86, no. 19, pp. 185–188, May 2005.

[6] M. R. Chowdhury, "An assessment of flood forecasting in Bangladesh: The experience of the 1998 Flood," *Nat. Hazards*, vol. 22, no. 2, pp. 139–163, Sep. 2000.

[7] J. E. Costa *et al.*, "Measuring stream discharge by non-contact methods: A proof-of-concept experiment," *Geophys. Res. Lett.*, vol. 27, pp. 553–556, Feb. 2000.

[8] M. Dewan, M. Nishigaki, and M. Komatsu, "Floods in Bangladesh: A comparative hydrological investigation on two catastrophic events," *J. Fac. Environ. Sci. Technol.*, vol. 8, no. 1, pp. 53–62, Mar. 2003.

[9] M. Durand, E. Rodriguez, D. E. Alsdorf, and M. Trigg, "Estimating river depth from remote sensing swath interferometry measurements of river height, slope, and width," *IEEE J. Sel. Topics Appl. Earth Observ.*, vol. 3, no. 1, pp. 20–31, Mar. 2010.

[10] M. Durand, K. Andreadis, Y. Yoon, and E. Rodriguez, "Sensitivity of SWOT discharge algorithm to measurement errors: Testing on the Sacramento River," in *Proc. EGU Gen. Assem.*, Vienna, Austria, Apr. 2013, vol. 15.

[11] A. Giacomelli, M. Mancini, and R. Rosso, "Assessment of flooded areas from ERS-1 PRI data: An application to the 1994 flood in Northern Italy," *Phys. Chem. Earth*, vol. 25, no. 5–6, pp. 469–474, 1995.

[12] F. Hossain and D. E. Alsdorf, "Understanding surface water flow and storage changes using satellites: Emerging opportunities for Bangladesh," in *Climate Change Flood Security in South Asia*, ch. 5. New York, NY, USA: Springer, 2011, pp. 57–67.

[13] F. Hossain, A. H. M. Siddique-E-Akbor, S. Biancamaria, H. Lee, and C. K. Shum, "Proof of concept of altimeter-based forecasting system for transboundary flooding," *IEEE J. Sel. Topics Appl. Earth Observ.*, vol. 7, no. 2, pp. 587–601, Feb. 2014, doi: 10.1109/JSTARS.2013.2283402.

[14] A. S. Islam, S. K. Bala, and M. A. Haque, "Flood inundation map of Bangladesh using MODIS time-series images," *J. Flood Risk Manage.*, vol. 3, no. 3, pp. 210–222, Sep. 2010.

[15] H.C. Jung *et al.*, "Characterization of complex fluvial systems using remote sensing of spatial and temporal water level variations in the Amazon, Congo, and Brahmaputra Rivers," *Earth Surf. Processes Landforms*, vol. 35, no. 3, pp. 294–304, Mar. 2010.

[16] M. Khalequzzaman, "Flood control in Bangladesh through best management practices," *Expatriate Bangladeshi 2000*, Short Note 17, 2000.

[17] V. Kouraev, E. A. Zakharovab, O. Samainc, N. M. Mognard, and A. Cazenave, "Ob' River discharge from TOPEX/Poseidon satellite altimetry (1992–2002)," *Remote Sens. Environ.*, vol. 93, pp. 238–245, Oct. 2004.

[18] H. L. Lee and L. W. Mays, "Hydraulic uncertainties in flood levee capacity," *J. Hydraul. Eng.*, vol. 112, no. 10, pp. 928–934, 1986.

[19] G. LeFavour and D. E. Alsdorf, "Water slope and discharge in the Amazon River estimated using the shuttle radar topography mission digital elevation model," *Geophys. Res. Lett.*, vol. 32, no. 17, Sep. 2005, article no. L17404.

Q4 [20] M. K. Mersel, L. C. Smith, K. M. Andreadis, and M. T. Durand, "Estimation of river depth from remotely sensed hydraulic relationships," *Water Resour. Res.*, vol. 49, pp. 3165–3179, doi: 10.1002/wrcr.20176.

[21] L. Moller-Jensen, "Knowledge-based classification of an urban area using texture and context information in Landsat-TM Imagery," *Photogramm. Eng. Remote Sens.*, vol. 56, no. 6, pp. 899–904, 1990.

[22] J. Neal *et al.*, "A data assimilation approach to discharge estimation from space," *Hydrol. Process.*, vol. 23, pp. 3641–3649, 2009.

Q5 [23] P. K. Parua, "Flood management in Ganga-Brahmaputra-Meghna basin: Some aspects of regional co-operation," *ASCE-IS*, Mar./Apr. 2003.

[24] P. K. Parua, "The Ganga's Hydrology," in *The Ganga: Water Use in the Indian Subcontinent*, ch. 4. New York, NY, USA: Springer, 2010, pp. 23–34.

[25] G. N. Paudyal, "Forecasting and warning of water related disasters in a complex hydraulic setting—The case of Bangladesh," *Hydrol. Sci. J.*, vol. 47(S), pp. S5–S18, Aug. 2002.

[26] R. Romeiser, J. Sprenger, D. Stammer, H. Runge, and S. Suchandt, "Global current measurements in rivers by spaceborne along-track InSAR," in *Proc. IEEE Int. Geosci. Remote Sens. Symp. (IGARSS'05)*, Jul. 2005, vol. 1.

[27] R. Rybushkina, "Validation of the retracked Jason l, 2-altimeter water levels over Gorky Reservoir of the Volga River," in *Proc. EGU Gen. Assem.*, Vienna, Austria, May 2010, vol. 12.

[28] G. Schumann, P. D. Bates, M. S. Horritt, P. Matgen, and F. Pappenberger, "Progress in integration of remote sensing-derived flood extent and stage data and hydraulic models," *Rev. Geophys.*, vol. 47, Nov. 2009.

[29] A. H. M. Siddique-E-Akbor, F. Hossain, H. Lee, and C. K. Shum, "Intercomparison study of water level estimates derived from hydrodynamic–hydrologic model and satellite altimetry for a complex deltaic environment," *Remote Sens. Environ.*, vol. 115, pp. 1522–1531, Jun. 2011.

[30] J. S. Silva *et al.*, "Water levels in the Amazon Basin derived from the ERS 2 and ENVISAT radar altimetry missions," *Remote Sens. Environ.*, vol. 114, no. 10, pp. 2160–2181, Oct. 2010.

[31] L. C. Smith, B. L. Isacks, A. L. Bloom, and A. B. Murray, "Estimation of discharge from three braided rivers using synthetic aperture radar (SAR) satellite imagery: Potential application to ungaged basins," *Water Resour. Res.*, vol. 32, pp. 2021–2034, Jul. 1996.

[32] L. C. Smith, "Satellite remote sensing of river inundation area, stage, and discharge: A review," *Hydrol. Process.*, vol. 11, pp. 1427–1439, 1997.

[33] Y. Wang, "Seasonal change in the extent of inundation on floodplains detected by JERS-1 Synthetic Aperture Radar data," *Int. J. Remote Sens.*, vol. 25, no. 13, pp. 2497–2508, Jul. 2004.

[34] A. T. Woldemichael, A. M. Degu, A. H. M. Siddique-E-Akbor, and F. Hossain, "Role of land–water classification and manning's roughness parameter in space-borne estimation of discharge for braided rivers: A case study of the Brahmaputra river in Bangladesh," *IEEE J. Sel. Topics Appl. Earth Observ.*, vol. 3, no. 3, pp. 395–403, Sep. 2010.

[35] O. Yoshiaki, I. Tadao, and I. Hideshige, "Time-series inundation mapping using RADARSAT-SAR," *J. Remote Sens. Soc. Jpn.*, vol. 20, no. 4, pp. 440–448, 2000.

Md. Safat Sikder received the B.S. degree in water resources engineering from Bangladesh University of Engineering and Technology, Dhaka, Bangladesh, and the M.S. degree from Tennessee Technological University, Cookeville, TN, USA, in 2013. Currently, he is pursuing the Ph.D. degree in civil and environmental engineering from the University of Washington, Seattle, WA, USA. Q6

His research interests include hydrologic and hydrodynamic modeling and application of remote sensing for surface water and flood forecasting.

Faisal Hossain received the B.S. and M.S. degrees from the Indian Institute of Technology, Varanasi, UP, India, and National University of Singapore, Singapore, respectively, and the Ph.D. degree from the University of Connecticut, Storrs, CT, USA, in 2004. Q7

Currently, he is an Associate Professor with the Department of Civil and Environmental Engineering, University of Washington, Seattle, WA, USA. He has published over 100 peer-reviewed journal articles, authored an undergraduate-level textbook, edited two book volumes, and contributed eight book chapters. His research interests include hydrologic remote sensing, uncertainty modeling of water cycle variables, human modification of extreme hydro-climatology, sustainable water resources engineering, spaceborne transboundary water resources management, engineering education, and public outreach.

Dr. Hossain is also a recipient of awards such as NASA New Investigator Award in 2008, National Association of Environmental Professionals Education Excellence Award in 2010, US Fulbright Faculty Award in 2012, Graduate Of the Last Decade (G.O.L.D.) award from the University of Connecticut in 2012, and American Geophysical Union (AGU) Charles Falkenberg Award in 2012.